Int. J. Electrochem. Sci., 10 **(2015)** 805 - 814

International Journal of
ELECTROCHEMICAL
SCIENCE
www.electrochemsci.org

Effect of Composition on the Structural and Electrochemical Properties of (1-x-y)Li[$Li_{1/3}Mn_{2/3}$]O_2-x$LiFeO_2$-y$LiNiO_2$ Solid Solution Cathode Materials

Jiangang Li[1,], Lei Wang[1], Yingzhuo Wang[1], Jianjun Li[2,3], Li Wang[2,4] and Xiangming He[2,4,*]*

[1] Beijing Institute of Petrochemical Technology, Beijing 102617, China
[2] Institute of Nuclear & New Energy Technology, Tsinghua University, Beijing 100084, China
[3] Huadong Institute of Lithium Ion Battery, Zhangjiagang, Jiangsu 215600, China
[4] State Key Laboratory of Automotive Safety and Energy, Tsinghua University, Beijing 100084
[*]E-mail: hexm@tsinghua.edu.cn; lijiangang@bipt.edu.cn

Received: 20 October 2014 / *Accepted:* 28 November 2014 / *Published:* 2 December 2014

Uniform solid solution of (1-x-y)Li[$Li_{1/3}Mn_{2/3}$]O_2-x$LiFeO_2$-y$LiNiO_2$ (x+y≤0.5) were prepared by citric acid assisted sol-gel process, and the effects of composition on the structural and electrochemical properties of as-prepared samples were investigated. The results indicate that all samples prepared at 650 °C ~ 800 °C show pure hexagonal phase. The composition has noticeable effects on structural properties such as interplaner spacing d_{003}, crystal particle size, crystallinity and 2D cation-ordering, thus affect electrochemical performance. Obvious cooperative effects are observed for the samples with suitable amount of composited $LiNiO_2$ and $LiFeO_2$ (x+y≈0.3~0.4). In view of capacity, cycling performance and cost, the samples with x+y≈0.3~0.4 and x/y=1.6~3.0 are considered to be more promising new cobalt-free cathode materials with high capacity of more than 240 $mAhg^{-1}$.

Keywords: Li-rich; Cobalt-free; Cathode; Lithium-ion batteries

1. INTRODUCTION

In recent years, new cathode materials with high capacity, low cost and environment friendly have been investigated thoroughly in order to fill the demands of Lithium-ion batteries for EV and HEV.[1] Among them the Ni- and Co- composited layered Li_2MnO_3-$LiMO_2$ (M = Ni, Co, $Ni_{1-x}Co_x$, $Ni_{0.5}Mn_{0.5}$, $Ni_{1/3}Co_{1/3}Mn_{1/3}$, $Mn_{0.5-y}Ni_{0.5-y}Co_{2y}$) solid solution materials attracted more attention of the researchers.[2-11]

In view of the cost and toxic elements in such Ni- and Co- composited layered Li_2MnO_3-$LiMO_2$ materials, cobalt free Li-rich cathode materials $LiFeO_2$-Li_2MnO_3 have been developed by

Tabuchi et al.[12-17] The $Li_{1+x}(Fe_yMn_{1-y})_{1-x}O_2$ solid solution ($0.3 \leq y \leq 0.5$) prepared by using a three-step preparation method including coprecipitation–hydrothermal–calcinations presented high capacity of >220 $mAhg^{-1}$. However, the cycleablity was poor due to the transformation of layered Li_2MnO_3 to spinel phase as well as the formation of inactive cubic $LiFeO_2$ phase. In order to improve the cycling stability, doping of $LiFeO_2$-Li_2MnO_3 was investigated by some research groups. Zheng et al. reported $Li(Li_{0.15}Ni_{0.21}Fe_{0.21}Mn_{0.45})O_2$ prepared by annealing the hydroxide co-precipitate precursor with excess LiOH (2 times).[18] The material exhibited excellent cycling performance, but its capacity only reached ~150 $mAhg^{-1}$, and too much LiOH also caused severe corrosion and difficulty of washing residual excess Li salt. Karthikeyan et al. reported another doped $LiFeO_2$-Li_2MnO_3 based solid solution with the composition of $Li_{1.2}(Mn_{0.32}Ni_{0.32}Fe_{0.16})O_2$. The material also showed good cycleablity but lower capacity (~160 $mAhg^{-1}$).[19] In order to develop a new composition of $LiFeO_2$-Li_2MnO_3 based solid solution, which can exceed the combined advantages of the existing cathodes with high capacity and stable cycleablity, our research group also developed a new cobalt free $LiFeO_2$-Li_2MnO_3 based solid solution with a composition of $Li(Li_{0.23}Mn_{0.47}Fe_{0.2}Ni_{0.1})O_2$.[20] The material, which was prepared by a new citric acid assisted sol-gel process including three-step of "preparation of wet gel—formation of spray-dried gel—annealing at high temperature", showed high capacity of 277.4 $mAhg^{-1}$ and better cycling stability. However, some important issues are still unclear. For example, how does the composition of Li_2MnO_3-$LiFeO_2$-$LiNiO_2$ affect the structural and electrochemical properties? Is there other composition except $Li(Li_{0.23}Mn_{0.47}Fe_{0.2}Ni_{0.1})O_2$ showing better Li-storage properties ?

In this study, we demonstrate the effects of solid solution composition on Li storage properties of $(1\text{-}x\text{-}y)Li[Li_{1/3}Mn_{2/3}]O_2$-$xLiFeO_2$-$yLiNiO_2$, and further optimize the solid solution composition to obtain the best electrochemical performance. For the purpose, a series of materials with the composition of $(1\text{-}x\text{-}y)Li[Li_{1/3}Mn_{2/3}]O_2$-$xLiFeO_2$-$yLiNiO_2$ ($x+y \leq 0.5$) were prepared by our proposed new sol-gel method.[20]

2. EXPERIMENTAL

The cathode materials $(1\text{-}x\text{-}y)Li[Li_{1/3}Mn_{2/3}]O_2$-$xLiFeO_2$-$yLiNiO_2$ were synthesized by our proposed citric acid assisted sol-gel process including three-step of "preparation of wet gel—formation of spray-dried gel—annealing at high temperature".[20] The transparent wet gel was prepared firstly by stirring and heating the solution containing stoichiometric quantities of $LiNO_3$, $Mn(NO_3)_2$, $Ni(NO_3)_2$, $Fe(NO_3)_3$ and citric acid (Citric aicid : Total metal amount = 1:1 by molar ratio) at 70 °C for 12 h. The wet gel was then spray-dried at the condition of inlet air temperature 180°C and outlet temperature 65 °C ~ 70 °C to form transparent yellow foam gel. The dried gel was heated at 400 °C for 5 h, and then annealed at 650 °C ~ 800 °C for 12 h followed by retreatment at 600 °C for 10 h in oxygen atmosphere to obtain products.

XRD-7000 X-ray Diffractometer was used to characterize the structure of $(1\text{-}x\text{-}y)Li[Li_{1/3}Mn_{2/3}]O_2$-$xLiFeO_2$-$yLiNiO_2$ powders. X-ray photoelectron spectroscopy (XPS) measurement was performed on an ESCALAB spectrometer (VG scientific) using a monochromic Al Kα light source.

The electrochemical characterization was performed using CR2032 coin cells. The cell consisted of a cathode with the composition of 86wt% (1-x-y)Li[$Li_{1/3}Mn_{2/3}$]O_2-x$LiFeO_2$-y$LiNiO_2$, 8wt% Super P carbon black, and 6wt% poly(vinylidenefluoride), and a lithium metal anode separated by a Celguard 2400 microporous film. All investigated cells featured cathode electrodes with 0.8 cm in diameter and an active area of 0.50 cm^2 respectively. The mass of active material in each cathode was about 5 mg. The electrolyte was 1 $molL^{-1}$ $LiPF_6$ /EC+DEC+DMC (1:1:1 by volume). The cells were assembled in an Etelux-Lab2000 glove box filled with pure argon. The charge-discharge tests were galvanostatically performed on LAND cell test system over 2.5~4.8 V at the current densities of 10 mAg^{-1}. AC-impedance measurements were performed using a Zahner Elektrik IM6 impedance analyzer over the frequency range from 100 KHz to 10 mHz with the amplitude of 5 mV.

3. RESULTS AND DISCUSSION

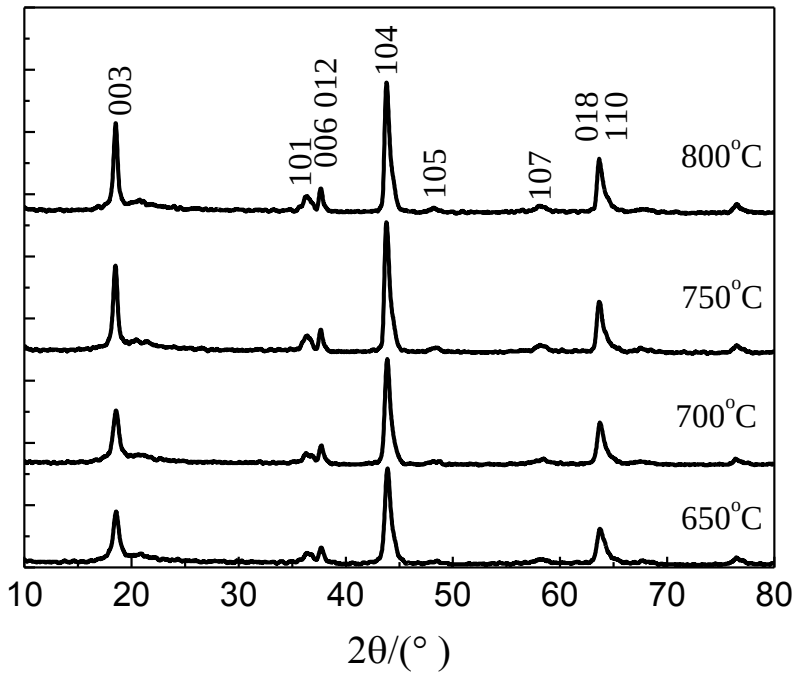

Figure 1. XRD patterns of 0.5Li[$Li_{1/3}Mn_{2/3}$]O_2-0.45$LiFeO_2$-0.05$LiNiO_2$ prepared at different temperature.

All of as-prepared products were investigated by XRD analysis. The results indicate that except for some weak peaks between 20° and 23°, all the diffraction peaks can be indexed based on a layered α-$NaFeO_2$-type structure, even for 0.5Li[$Li_{1/3}Mn_{2/3}$]O_2-0.45$LiFeO_2$-0.05$LiNiO_2$ sample with high content of $LiFeO_2$, as shown in Fig. 1. The weak peaks between 20° and 23° are considered to be attributed to the superlattice ordering of Li and Mn in the transition-metal layers of Li_2MnO_3.[21] No impurity phases like $LiMnO_2$ and α-$LiFeO_2$ can be detected, which indicates that the formation of cubic $LiFeO_2$ can be suppressed by the composited Li_2MnO_3. It can be speculated that uniform solid

solution of (1-x-y)Li[$Li_{1/3}Mn_{2/3}$]O_2-x$LiFeO_2$-y$LiNiO_2$ (x+y≤0.5) with pure hexagonal phase (or monoclinic phase) is prepared at 650 °C ~ 800 °C in the work.

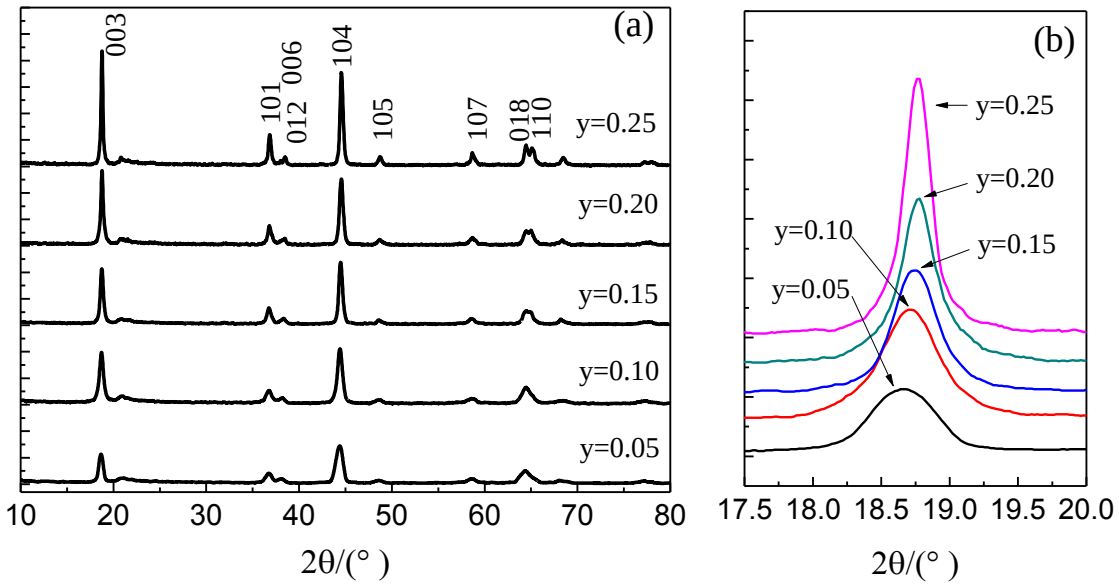

Figure 2. XRD patterns (a) and the corresponding (003) diffraction peaks (b) of 0.7Li[$Li_{1/3}Mn_{2/3}$]O_2-(0.3-y)$LiFeO_2$-y$LiNiO_2$ prepared at 700°C.

0.7Li[$Li_{1/3}Mn_{2/3}$]O_2-(0.3-y)$LiFeO_2$-y$LiNiO_2$ was selected to carry on further XRD analysis in order to investigate the effect of solid solution composition on the structure of (1-x-y)Li[$Li_{1/3}Mn_{2/3}$]O_2-x$LiFeO_2$-y$LiNiO_2$. The results are shown in Fig. 2. Fig. 2a shows that increasing $LiNiO_2$ content in the investigated solid solution results in enhanced splitting of (006)/(102) and (018)/(110) doublets, and increasing of I_{003}/I_{104}. It suggests that increasing $LiNiO_2$ content leads to the improvement of the 2D cation-ordering layered structure of 0.7Li[$Li_{1/3}Mn_{2/3}$]O_2-(0.3-y)$LiFeO_2$-y$LiNiO_2$ samples, which is beneficial for Li^+ diffusion along (003) lattice plane. Further analysis of (003) diffraction peaks, as shown in Fig. 2b, reveals that increasing $LiFeO_2$ content make (003) diffraction peak broaden and shift to low 2θ angle, indicating that increasing $LiFeO_2$ content can enlarge interplaner spacing d_{003}, decrease crystal particle size and shorten Li^+ diffusion path. It displays that increasing $LiFeO_2$ content in 0.7Li[$Li_{1/3}Mn_{2/3}$]O_2-(0.3-y)$LiFeO_2$-y$LiNiO_2$ samples make the 2D cation-ordering decrease, but enlarged interplaner spacing d_{003} and shorten Li^+ diffusion path may provide a possibility for improving the electrochemical properties.

Fig. 3 shows the Mn-, Fe- and Ni-2p XPS spectra of 0.7Li($Li_{1/3}Mn_{2/3}$)O_2-0.2$LiFeO_2$-0.1$LiNiO_2$ samples prepared at different temperatures. The Ni $2p_{3/2}$ binding energy of the samples center at 854.9 eV, which is a little smaller than that of Ni^{3+} in $LiNiO_2$ [22] but obvious higher than that of Ni^{2+} in NiO [23]. It indicates that nickel ions in the samples exist mainly in an oxidation state of Ni^{3+}. Small part of Ni^{2+} may come from NiO which has been reported to be formed on the surface of the nickel-containing metal oxides while stored in air.[24] The Mn $2p_{3/2}$ binding energy locates at 642.1 eV. This is consistent with that of Mn^{4+} reported in literatures.[25, 26] The Fe $2p_{3/2}$ binding energy was 710.6 eV,

which agrees well with that of Fe^{3+} in γ-Fe_2O_3,[27] confirming the +3 oxidation state of Fe in the samples. All of investigated samples prepared under same atmosphere (O_2) show almost same binding energy, therefore, the valence states of Mn, Fe and Ni in our prepared samples present +4, +3 and +3, respectively.

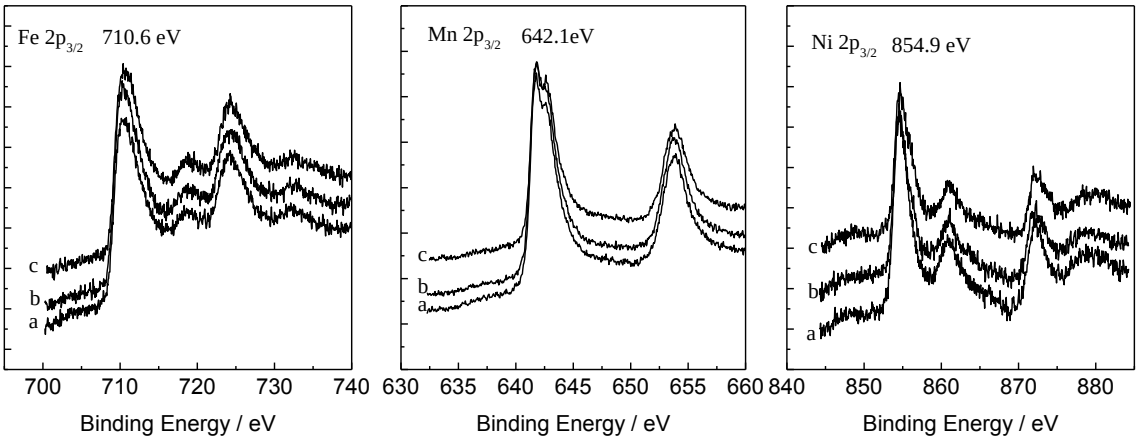

Figure 3. XPS patterns of 0.7Li($Li_{1/3}Mn_{2/3}$)O_2-0.2$LiFeO_2$-0.1$LiNiO_2$ annealed at 600℃ (a), 700℃ (b), and 800℃ (c).

Table I. Charge-discharge properties of (1-x-y)Li[$Li_{1/3}Mn_{2/3}$]O_2-x$LiFeO_2$-y$LiNiO_2$

Composition	1st discharge capacity (Q_{1d}) / $mAhg^{-1}$	10th discharge capacity (Q_{10d}) / $mAhg^{-1}$	Capacity retention (Q_{10d}/Q_{1d}) / %
x=0.05 y=0.05	305	115	37.7
x=0.15 y=0.05	233	175	75.1
x=0.10 y=0.10	320	155	48.4
x=0.05 y=0.15	262	173	66.0
x=0.25 y=0.05	257	220	85.6
x=0.20 y=0.10	277	269	97.1
x=0.15 y=0.15	214	207	96.7
x=0.10 y=0.20	232	220	94.8
x=0.05 y=0.25	262	212	80.9
x=0.35 y=0.05	190	178	93.7
x=0.30 y=0.10	245	195	79.7
x=0.25 y=0.15	247	198	80.2
x=0.20 y=0.20	211	177	83.9
x=0.15 y=0.25	212	171	80.7
x=0.10 y=0.30	217	185	85.2
x=0.05 y=0.35	236	207	87.7
x=0.45 y=0.05	166	136	81.9
x=0.40 y=0.10	168	138	82.1
x=0.35 y=0.15	179	135	75.4
x=0.30 y=0.20	160	140	87.5
x=0.25 y=0.25	165	141	85.4
x=0.20 y=0.30	153	138	89.6
x=0.15 y=0.35	174	119	68.4
x=0.10 y=0.40	200	163	81.5
x=0.05 y=0.45	203	146	71.9

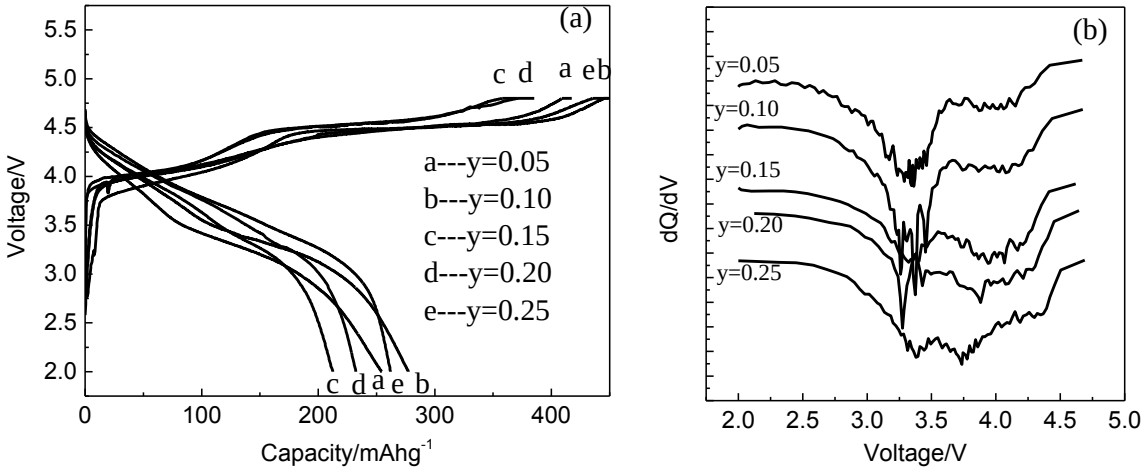

Figure 4. The first charge-discharge curves (a) and the corresponding differential discharge capacity (dQ/dV) vs. voltage curves (b) of the $0.7Li[Li_{1/3}Mn_{2/3}]O_2$-$(0.3-y)LiFeO_2$-$yLiNiO_2$ prepared at 700 °C.

The Li-storage properties of as-prepared $(1-x-y)Li[Li_{1/3}Mn_{2/3}]O_2$-$xLiFeO_2$-$yLiNiO_2$ samples were investigated by charge-discharging during 2.0~4.8 V at constant current of 10 mAg^{-1} for 10 cycles. The results are summarized in Table I. As an example, Fig. 4 presents the first charge-discharge curves and the corresponding differential discharge capacity (dQ/dV) vs. voltage curves of $0.7Li[Li_{1/3}Mn_{2/3}]O_2$-$(0.3-y)LiFeO_2$-$yLiNiO_2$ prepared at 700 °C. As shown in Fig. 4a, two different plateaus are observed below and above 4.4 V in the charge curves. The charge curves below 4.4 V have been attributed to Li extraction from $LiMO_2$ component accompanied by the reaction of Ni^{3+}/Ni^{4+} and Fe^{3+}/Fe^{4+} redox couple, and that above 4.4 V to an oxidation of O^{2-} ions and Li_2O extraction from Li_2MnO_3 component, respectively.[5, 12-17, 21, 28] For the discharge curves in Fig. 4a, no obvious plateau above 4.4 V is observed due to the irreversible reaction of Li_2O extraction from Li_2MnO_3 component, which causes large irreversible capacity loss. In order to further explore the charge-discharge mechanism during the first cycle, the differential discharge capacity (dQ/dV) vs. voltage curves of $0.7Li[Li_{1/3}Mn_{2/3}]O_2$-$(0.3-y)LiFeO_2$-$yLiNiO_2$ were compared in Fig. 4b. It can be seen that with increasing $LiNiO_2$ content, the capacity below 3.5 V drop off, and the capacity above 3.5 V increase gradually. For example, compared with the sample y=0.10, the sample y=0.25 shows a close discharge capacity but an obvious increased peak around 3.75 V corresponding to the reduction of Ni^{4+}.[29] Above results indicate that all of transition metal ions in $(1-x-y)Li[Li_{1/3}Mn_{2/3}]O_2$-$xLiFeO_2$-$yLiNiO_2$ participate in the electrochemical redox reaction during the charge-discharge process, and increasing $LiNiO_2$ content is beneficial for elevation of discharge voltage plateau.

The effects of solid solution composition on the electrochemical performance of $(1-x-y)Li[Li_{1/3}Mn_{2/3}]O_2$-$xLiFeO_2$-$yLiNiO_2$ are shown in Fig. 5. In the figure, the listed data are the first discharge capacity, and the capacity retention with ≥90%, 80~89%, 65~79% and <65% after 10 cycles is defined as excellent cycleablity, good cycleablity, moderate cycleablity and poor cycleability, respectively. It can be seen that although increasing $Li[Li_{1/3}Mn_{2/3}]O_2$ content can improve the discharge capacity, too much $Li[Li_{1/3}Mn_{2/3}]O_2$ ($x+y\leq0.2$) leads to poor cycle stability, which can be

attributed to the structure transformation from layer to spinel-like.[30, 31] However, the samples with suitable amount of $LiNiO_2$ and $LiFeO_2$ (x+y≈0.3~0.4) can present high capacity of >210 $mAhg^{-1}$ and good cycling performance, as shown in shadow area of Fig. 5.

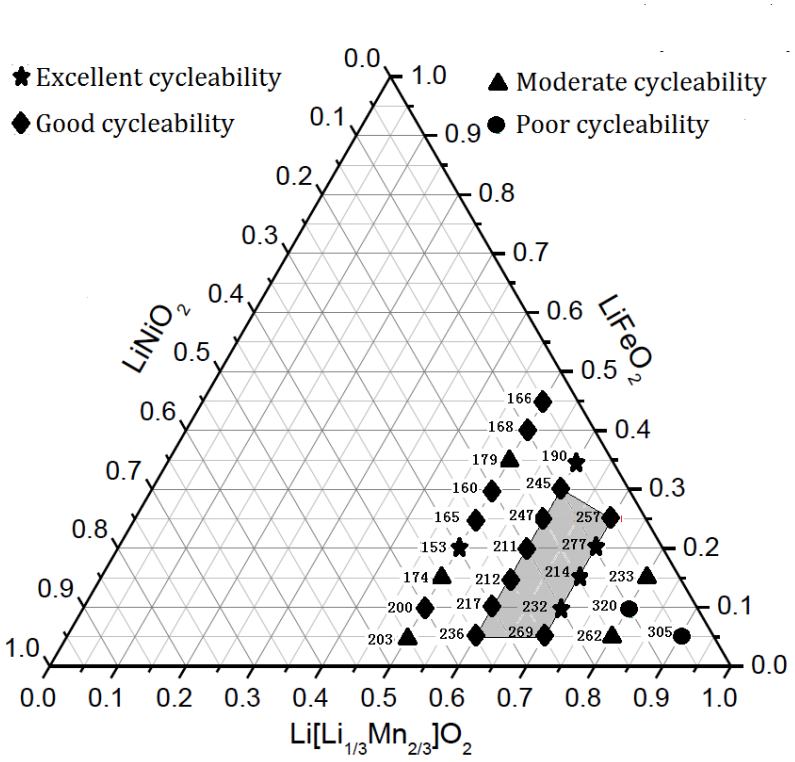

Figure 5. Effect of composition on the electrochemical performance of (1-x-y)$Li[Li_{1/3}Mn_{2/3}]O_2$-x$LiFeO_2$-y$LiNiO_2$.

It implies that suitable amounts of composited $LiFeO_2$ and $LiNiO_2$ in the solid solution is beneficial for reducing the transformation of layered $Li[Li_{1/3}Mn_{2/3}]O_2$ to spinel phase, and suitable amounts of composited $Li[Li_{1/3}Mn_{2/3}]O_2$ can also restrain cubic $LiFeO_2$ formation. Obvious cooperative effects are observed. In addition, for samples with x+y=0.3~0.5, an interesting phenomena is observed that the sample with x≈y show lower capacity than ones with x/y≤0.6 or x/y=1.6~3.0. In order to clarify the reason, AC-impedance analysis was carried out, and the results are shown in Fig.6. For sample with y=0.05, 0.10, 0.15, 0.20 and 0.25, the charge transfer resistance R_{ct} are simulated to be 793.5 Ω, 175.8 Ω, 780.2 Ω, 361.8 Ω and 119.0 Ω respectively, and the Li^+ diffusion coefficient D_{Li}^+ are calculated to be 2.34×10^{-16} cm^2s^{-1}, 1.47×10^{-15} cm^2s^{-1}, 9.10×10^{-16} cm^2s^{-1}, 1.06×10^{-15} cm^2s^{-1} and 1.38×10^{-15} cm^2s^{-1} respectively based on the low frequency line data.[32, 33] Compared with the sample y=0.15, the sample y=0.10 shows smaller R_{ct} and higher D_{Li}^+ value, which is consist with its higher capacity. In view of its lower cation-ordering, it is speculated that its larger interplaner spacing d_{003} and shorter Li^+ diffusion path due to small crystal particle size may contribute to its better Li^+ intercalation-deintercalation properties. However, the sample y=0.20 and 0.25 also shows smaller R_{ct}, higher D_{Li}^+ and higher capacity in spite of longer Li^+ diffusion path due to higher crystal particle size. That may be attributed to its higher cation-ordering 2D layered structure. Although further studies on

the mechanism of this aspect are still needed in the future, it is very meaningful that as compared with reported other $LiFeO_2$-Li_2MnO_3 based solid solution materials,[12-19] our prepared samples (1-x-y)$Li[Li_{1/3}Mn_{2/3}]O_2$-x$LiFeO_2$-y$LiNiO_2$ with x+y≈0.3~0.4 and x/y=1.6~3.0 exhibit the combined advantages of high capacity, good cycling stability and low cost, which can be considered as more promising new cobalt-free cathode materials with high capacity of more than 240 $mAhg^{-1}$.

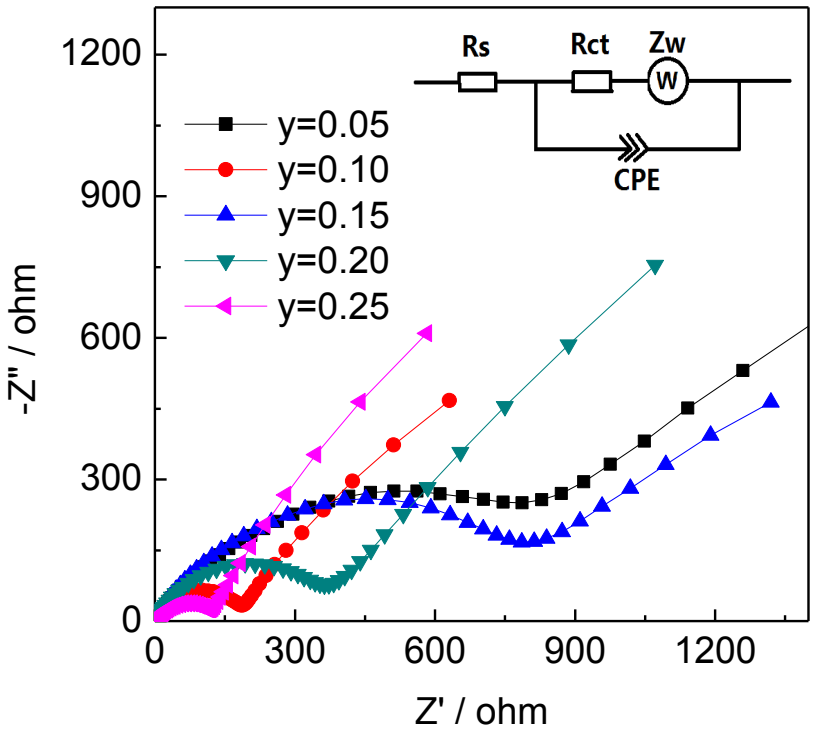

Figure 6. AC impedance patterns of 0.7$Li[Li_{1/3}Mn_{2/3}]O_2$-(0.3-y)$LiFeO_2$-y$LiNiO_2$ prepared at 700°C.

4. CONCLUSION

Uniform solid solution of (1-x-y)$Li[Li_{1/3}Mn_{2/3}]O_2$-x$LiFeO_2$-y$LiNiO_2$ (x+y≤0.5) with pure hexagonal phase (or monoclinic phase) can be prepared at 650 °C ~ 800 °C by citric acid assisted sol-gel process including three-step of "preparation of wet gel—formation of spray-dried gel—annealing at high temperature". Suitable amounts of composited $Li[Li_{1/3}Mn_{2/3}]O_2$ in the solid solution can improve the discharge capacity and also restrain cubic $LiFeO_2$ formation, suitable amounts of composited $LiFeO_2$ and $LiNiO_2$ is beneficial for reducing the transformation of layered $Li[Li_{1/3}Mn_{2/3}]O_2$ to spinel phase. Increasing $LiFeO_2$ content can enlarge interplaner spacing d_{003}, decrease crystal particle size and shorten Li^+ diffusion path, but increasing $LiNiO_2$ content can increase crystallinity and 2D cation-ordering of the layered structure of 0.7$Li[Li_{1/3}Mn_{2/3}]O_2$-(0.3-y)$LiFeO_2$-y$LiNiO_2$ samples. Obvious cooperative effects are observed for the samples with suitable amount of $LiNiO_2$ and $LiFeO_2$ (x+y≈0.3~0.4), which can present high capacity of >210 $mAhg^{-1}$ and good cycling performance. In view of capacity, cycling performance and cost, the samples with x+y≈0.3~0.4 and

x/y=1.6~3.0 are considered to be more promising new cobalt-free cathode materials with high capacity of more than 240 $mAhg^{-1}$.

ACKNOWLEDGEMENTS
This work is supported by Beijing Natural Science Foundation (Grant No. 2122016) , the MOST (Grant No. 2013CB934000, No. 2011CB935902, No. 2014DFG71590, No. 2013AA050903, No. 2011AA11A257 and No. 2011AA11A254), the Tsinghua University Initiative Scientific Research Program (Grant No. 2011THZ08139, No. 2011THZ01004 and No. 2012THZ08129) , Beijing Municipal Program (Grant No. YETP0157, No. Z131100003413002 and No. Z131100003413001) and State Key Laboratory of Automotive Safety and Energy (No. ZZ2012-011), Suzhou (Wujiang) Automotive Research Institute (Project No.2012WJ-A-01).

References

1. J.W. Fergus, Recent developments in cathode materials for lithium ion batteries, *J. Power Sources*, 195 (2010) 939.
2. Z. Lu, J.R. Dahn, *J. Electrochem. Soc.*, 149 (2002) A1454.
3. C.W. Park, S.H. Kim, K.S. Nahm, H.T. Chung, Y.S. Lee, J.H. Lee, S. Boo, J. Kim, *J. Alloy Compds*., 449 (2008) 343.
4. J.-M. Kim, S. Tsuruta, N. Kumagai, *Electrochem. Comm*., 9 (2007) 103.
5. M.M. Thackeray, S.-H. Kang, C.S. Johnson, J.T. Vaughey, R. Benedek and S.A. Hackney, *J. Mater. Chem*., 17 (2007) 3112.
6. Y. Sun, C. Ouyang, Z. Wang, X. Huang, and L. Chen, *J. Electrochem. Soc*., 151 (2004) A504.
7. P.S. Whitfield, S. Niketic, I.J. Davidson, *J. Power Sources*, 146 (2005) 617.
8. L. Zhang, K. Takada, N. Ohta, K. Fukuda, T. Sasaki, *J. Power Sources*, 146 (2005) 598.
9. N. Yabuuchi, K. Yoshii, S.T. Myung, I. Nakai, S. Komaba, *J. Am. Chem. Soc*., 133(2011) 4404.
10. J.-H. Lim, H. Bang, K.-S. Lee, K. Amine, Y.-K. Sun, *J. Power Sources*, 189 (2009) 571.
11. Y. Wu, A. Manthiram, *Solid State Ionics*, 180 (2009) 50.
12. M. Tabuchi, H. Shigemura, K. Ado, H. Kobayashi, H. Sakaebe, H. Kageyama, R. Kanno, *J. Power Sources*, 97-98 (2001) 415.
13. M. Tabuchi, A. Nakashima, K. Ado, H. Sakaebe, H. Kobayashi, H. Kageyama, K. Tatsumi, Y. Kobayashi, S. Seki, A. Yamanaka, *J. Power Sources*, 146 (2005) 287.
14. M. Tabuchi, A. Nakashima, K. Ado, H. Kageyama, and K. Tatsumi, *Chem. Mater*., 17 (2005) 4668.
15. M. Tabuchi, Y. Nabeshima, K. Ado, M. Shikano, H. Kageyama, K. Tatsumi, *J. Power Sources*, 174 (2007) 554.
16. M. Tabuchi, Y. Nabeshima, K. Ado, M. Shikano, H. Kageyama, K. Tatsumi, *J. Power Sources*, 195 (2010) 834.
17. J. Kikkawa, T. Akita, M. Tabuchi, M. Shikano, K. Tatsumi, and M. Kohyama, *J. Appl. Phys*., 103 (2008) 104911.
18. X. Zheng, L. Cao, W. Zhu, X. Qiu, *Acta Chimica Sinica*, 65 (2007) 571.
19. K. Karthikeyan, S. Amaresh, G.W. Lee, V. Aravindan, H. Kim, K.S. Kang, W.S. Kim, Y.S. Lee, *Electrochim. Acta*, 68 (2012) 246.
20. J. Li, L. Wang, L. Wang, J. Luo, J. Gao, J. Li, J. Wang, X. He, G. Tian, S. Fan, *J. Power Sources*, 244 (2013) 652.
21. A.R. Armstrong, M. Holzapfel, P. Novak, C.S. Johnson, S.H. Kang, M.M. Thackeray, P.G. Bruce, *J. Am. Chem. Soc*., 128 (2006) 8694.
22. M.E. Spahr, P. Novak, B. Schnyder, O. Haas, R. Nespar, *J. Electrochem. Soc*., 145 (1998) 1113.

23. S.H. Kang, J. Kim, M.E. Stoll, D. Abraham, Y.K. Sun, K. Amine, *J. Power Sources*, 112 (2002) 41.
24. A.W. Moses, H. G. G. Flores, J.-G. Kim, M. A. Langell, *Applied Surface Science*, 253 (2007), 4782.
25. E. Regan, T. Groutso, J. B. Metson, R. Steiner, B. Ammundsen, D. Hassell and P. Pickering, *Surf. Interface Anal*., 27 (1999) 1064.
26. R.J. Iwanowski, M.H Heinonen, E Janik, *Chem. Phys. Lett*., 387 (2004) 110.
27. A.C. Garade, M. Bharadwaj, S.V. Bhagwat, A.A. Athawale, C.V. Rode, *Catal. Commun*., 10 (2009) 485.
28. Z. Lu, J.R. Dahn, *J. Electrochem. Soc*., 149 (2002) A815.
29. S. Yang, X. Wang, X. Yang, Y. Bai, Z. Liu, H. Shu, Q. Wei, *Electrochimica Acta*, 66 (2012) 88.
30. A.D. Robertson, P. G. Bruce, *Chem. Mater*., 15 (2003) 1984.
31. D.Y.W. Yu, K. Yanagida, Y. Kato, H. Nakamura, *J. Electrochem. Soc*., 156 (2009) A417.
32. Q. Zhuang, S. Xu, X. Qiu, Y. Cui, L. Fang, S. Sun, *Progress in Chemistry* (Chinese), 22 (2010) 1044.
33. R. Shalini, N. Munichandraiah, A.K. Shukla, *J. Power Sources*, 87 (2000) 12.